



Hyperspectral near-infrared imaging for the detection of physical damages of pear



Wang-Hee Lee^a, Moon S. Kim^b, Hoonsoo Lee^a, Stephen R. Delwiche^c, Hanhong Bae^d, Dae-Yong Kim^a,
Byoung-Kwan Cho^{a,*}

^a Department of Biosystems Machinery Engineering, Chungnam National University, Daejeon 305-764, South Korea

^b Environmental Microbial and Food Safety Laboratory, Agricultural Research Service, USDA, Beltsville, MD 20705, USA

^c Food Quality Laboratory, Agricultural Research Service, USDA, Beltsville, MD 20705, USA

^d School of Biotechnology, Yeungnam University, Gyeongsan 712-749, South Korea

ARTICLE INFO

Article history:

Received 23 August 2013

Received in revised form 26 December 2013

Accepted 30 December 2013

Available online 9 January 2014

Keywords:

Hyperspectral imaging

F-value classification algorithm

Image processing

Near infrared spectrum

Pear bruise

ABSTRACT

Bruise damage on pears is one of the most crucial internal quality factors, which needs to be detected in postharvest quality sorting processes. Near-infrared imaging techniques (NIR) have effective potentials for identifying and detecting bruises since bruises result in the rupture of internal cell walls due to defects on agricultural materials. In this study, a novel NIR technique, hyperspectral imaging with beyond NIR range of 950–1650 nm, was investigated for detecting bruise damages underneath the pear skin, which has never been examined in the past. A classification algorithm based on *F*-value was applied for analysis of image to find the optimal waveband ratio for the discrimination of bruises against sound surface. The result demonstrated that the best threshold waveband ratio detected bruises with the accuracy of 92%, illustrating that the hyperspectral infra-red imaging technique with the region beyond NIR could be a potential detection method for pear bruises.

© 2014 Elsevier Ltd. All rights reserved.

1. Introduction

Optical sensing and imaging technologies have been an effective tool for non-destructive inspection and assessment for quality and safety of agricultural/food products. For fruits, NIR spectral imaging is one of the most successful methods for detecting damages in the products, and recent advance in spectroscopic device allows developing innovative technique collecting information which cannot be obtained by conventional methods.

Recently, a novel method that integrates two mature technologies of imaging and spectroscopy, named hyperspectral image, has been developed and increasingly used for non-destructive evaluation of fruit quality. Hyperspectral sensing technique, also known as chemical imaging, collects image data at a series of narrow and contiguous wavelength bands, acquiring both spatial and spectral information simultaneously. The obtained data forms a three dimensional hyperspectral cube which consists of two dimensional spatial images with additional spectral information. The spectrum of each spatial pixel contains fingerprints or signatures of substances at corresponding spot on the hyperspectral image. As hyperspectral imaging can report both chemical and physical information of the material, it provides an opportunity for more

detail image analysis which makes it possible to discriminate either visually indistinguishable defects or spectrally similar materials. This novel technique was initially implemented for remote sensing applications which utilize satellite imaging data of planets such as mineral mapping (Clark et al., 1992), soil property detection (Ben-Dor et al., 2002), and vegetation mapping (Aber and Martin, 1995), but broaden its application to diverse fields of agriculture, pharmaceuticals and medical science.

Because hyperspectral imaging is applicable for large spatial sampling areas, it can be used for scanning the whole products, potentiating it as an effective tool for identifying and detecting spectral and spatial anomalies on agricultural products. Limitations of manual sorting and classical imaging technique, such as inefficiency, low accuracy, and labor and time-intensive nature, have launched the hyperspectral imaging in detecting fruit defects. Particularly, its high-sensitivity detecting indistinctive defects in agricultural products is fit for sensing bruise damage on fruits which deteriorates fruit quality, costing significant economic losses.

One of the earlier studies using NIR hyperspectral imaging technique was to investigate detection of bruises on Red Delicious and Golden Delicious apples (Lu, 2003). This study developed a suitable system for using an extended NIR range. It reports that reflectance of bruised damages increased over time in the spectral range between 1000 nm and 1340 nm corresponding to the most appropriate range for bruise detection with 54–94% of correct detection rate. Other researchers have also used hyperspectral image in the

* Corresponding author. Address: 99 Deahak-ro(St.), Yuseong-gu, Daejeon 305-764, South Korea. Tel.: +82 42 821 6715; fax: +82 42 823 6246.

E-mail address: chobk@cnu.ac.kr (B.-K. Cho).

400–1000 nm region analyzed by statistical methods to detect bruises on 'Jonagold' apples after 1 day with an accuracy of 77.5% (Xing and De Baerdemaeker, 2005, 2007), and free formed bruises on 'Golden Delicious' with 86% accuracy (Xing et al., 2007). Similar application of hyperspectral imaging with the use of three NIR spectral bands at 750, 820, 960 nm was proposed for successful discrimination of bruised 'McIntosh' apples (ElMasry et al., 2008). Recently, 'Fuji' apples were studied using hyperspectral imaging technique to discriminate bruises with a classification threshold calculated by two-band ratio (Cho et al., 2011). Besides apples, damages on other fruits have been examined. Pits in tart cherries were optimally identified with spectral region between 692 and 856 nm in hyperspectral imaging (Qin and Lu, 2005), and a portable hyperspectral imaging device was utilized for detecting canker lesions on citrus fruit in the wavelength range between 400 and 900 nm (Qin et al., 2008). For detecting invisible bruises on 'Crystal' pears, four different classification algorithms were applied into hyperspectral image data collected with the spectral range of 408–1117 nm to compare classification accuracies (Zhao et al., 2010). Recent study on kiwifruit demonstrated that bruises on kiwifruit are detectable using 5 optimal wavelengths in the Vis/NIR hyperspectral image (Lu et al., 2011). Recently, a study has reviewed hyperspectral imaging technique in evaluating fruit and vegetable quality (Lorente et al., 2012).

It has been reported that internal quality of fruits is more effectively detected by an extended region beyond Vis/NIR (Lu et al., 2000; Moons et al., 1998). Nevertheless, few studies have been used NIR because of the lack of suitable NIR imaging devices covering the extended NIR region (Lu, 2003). Moreover, to our knowledge, only hyperspectral Vis/NIR imaging have been used to detect bruises on pears, but the extended range of NIR has not been used (Zhao et al., 2010), promoting the originality of this study using the extended range of NIR for pear bruise detection.

In this study, near infrared hyperspectral imaging in the 950–1650 nm region was firstly used to investigate the feasibility of multispectral reflectance ratio imaging techniques for detection of bruise damages on 'Shingo' pear. Simple ANOVA classification, a novel way to analyze hyperspectral imaging, was explored to select waveband ratio and threshold values for optimal classification of bruised pears (Cho et al., 2011). Findings in this study is expected to potentially propose developing low-cost and real-time multispectral imaging systems for quality sorting of pear in fruit processing plants.

2. Materials and methods

2.1. Fruits and bruising

'Shingo' pears were purchased from a local market in February 2011. For bruise treatments, two bruises spots in the middle area between stem and calyx on four individual pears were created by dropping the fruits. Three bruise levels were created using 5, 10 and 15 cm dropping heights. A total of 14 samples, four pears for each of three levels of bruise treatments, and two pears as control, were evaluated in this investigation. Hyperspectral images of pears were acquired before and after bruise treatments – measurements were conducted 1 h after the initial bruising, followed by 1, 2, 3, 4, 7, 9, and 11 days. For the duration of this hyperspectral imaging study, the sample pears were stored under ambient conditions (20 °C and 30% RH).

2.2. Hyperspectral imaging system

A schematic diagram of the hyperspectral NIR imaging system and form of three dimensional hyperspectral data are illustrated

in Fig. 1. It consists of a 320 (spatial) × 256 (spectral) pixel InGaAs Focal Plane Array (FPA) camera (Xenics, Model XEVA-1.7-320, 14-bit, Leuven, Belgium), an imaging spectrograph (SWIR Hyperspec, Headwall photonics, Fitchburg, MA, USA), and a 25-mm focal length lens (Optec, Model OB-SWIR25/2, Parabiago, Italy) along with a computer-controlled uniaxial stage (Velmex, Model XN10-0180-M02-21, Velmex Inc., Bloomfield, NY, USA). The spectrograph disperses incoming radiation from each spatial location on the line scan. The sample is scanned line-by-line over a nominal wavelength range of approximately 950–1650 nm. The use of a programmable positioning table allows line-by-line sample imaging for reflectance measurements. For each line scan measurement, the positioning table was incremented by 0.5 mm at an exposure time of 15 ms. The full hyperspectral image was acquired in about 110 s with 250 scans for a pear.

Illumination for reflectance imaging is provided by two 150 W quartz tungsten halogen lamps (Dolan Jenner, Model DC-950, MA, USA) and the lights are conveyed through low-OH fiber assemblies (1 m length, Dolan Jenner), with one end of the assembly coupled to the lamp enclosure and the other end arranged in a thin line (250 mm) of fibers. Two fiber assemblies are used to illuminate the line of IFOV (instantaneous field of view) of the imaging system, with the line of fibers positioned 75 mm above the IFOV at 10° forward and backward angle with respect to the vertical to illuminate the IFOV. Except for the QTH lamp box, imaging system

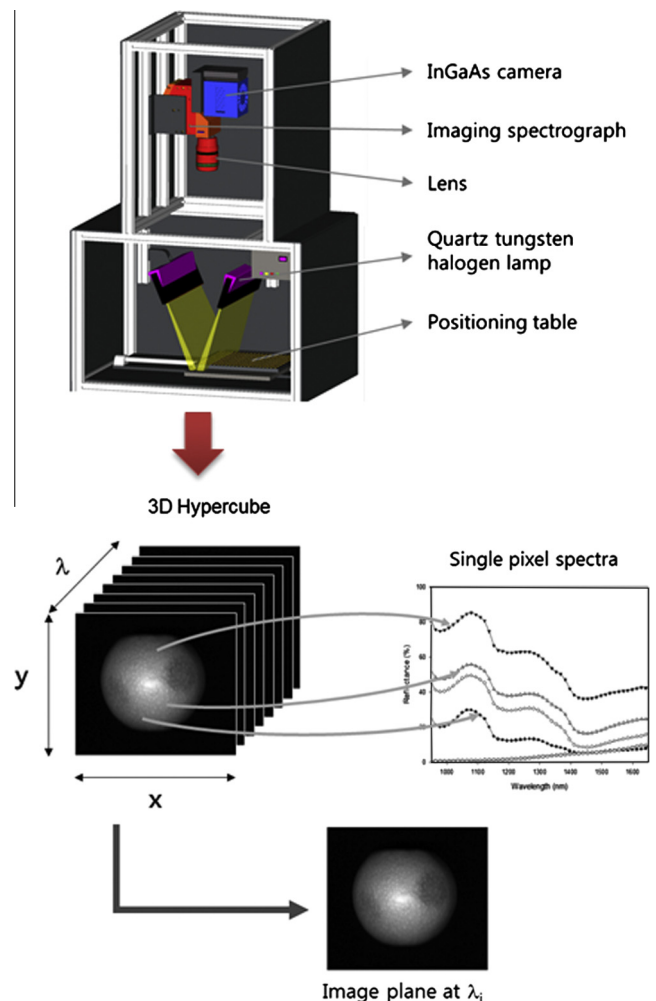


Fig. 1. Schematic illustration of NIR (950–1650 nm) hyperspectral reflectance imaging system and hypercube structure; spatial axes x , y , and spectral axis λ .

Download English Version:

<https://daneshyari.com/en/article/223069>

Download Persian Version:

<https://daneshyari.com/article/223069>

[Daneshyari.com](https://daneshyari.com)